Semiflexible Polymer Brushes: Most Probable Configuration Approach Based on Cotinuous Chain Model

Gwang Gyu Kim and Kookheon Char*

Division of Chemical Engineering, Seoul National University, Seoul 151-742, Korea
Received May 1, 1999

The properties of semiflexible polymer brushes are studied by applying the classical limit of mean-field approach for chains with marginal chain stiffness. Using the mean-spherical Gaussian model, the most probable configuration for semiflexible chains is obtained, which reduces to the parabolic brush of Milner *et al.* [*Macromolecules* **1988**, 21, 2610] in the flexible limit. From this configuration, equilibrium brush height as well as interactions between semiflexible brushes are estimated.

Introduction

Polymer chains with one ends tethered to an interface or a surface with high attachment density form polymer brushes.[1,2] The polymer brushes in solution, showing quite different properties from free polymer chains in that they exhibit deformed configuration even in equilibrium condition due to the excluded volume effect, become a basic model for a variety of polymeric systems such as polymeric surfactants, stabilization of colloidal dispersions, and wetting properties of surfaces and adhesion. The unique structure of the polymer brushes has thus motivated a number of experimental and theoretical studies. One of the most important applications of the polymer brushes is the colloid stablilization by end-tethered chains.[3-5] When the coverage of end-tethered chains is low and poor solvent is used, solid colloid particles may flocculate but as the grafting density is increased and solvent quality is improved, the polymer brushes separate colloidal particles to a distance at which van der Waals interaction is too weak to keep the particles together due to the repulsive force between the brushes arising from high osmotic pressure inside the brushes.

Pioneering work on polymer brushes was given by Alexander[6] and de Gennes.[7] Their equilibrium brush theory assuming uniformly stretched chains with a simple step function profile is based upon a free energy balance argument. By balancing the osmotic pressure resulting from excluded volume interaction of the brushes with the elastic stretching forces of elongation favoring to have maximum configurational entropy, they obtained $h \sim N(\omega\sigma l^2)^{1/3}$, $f \sim N(\omega\sigma/l)^{2/3}$ where h is brush height, f is the free energy of a chain in brush phase, N is the number of brush repeating units, σ is the surface density, ω is the excluded volume parameter and l is the statistical segment length. Their original work has prompted a large body of literature dealing with different approaches such as the self-consistent field equation first developed by Dolan and Edwards,[4] scaling approach[7] and more recently computer simulations.[8-10] Previous studies, however, mostly focused on flexible polymer brushes and few studies have reported on *semiflexible* polymer brushes.

Most real polymer chains possess inherent backbone rigidity.[11-13] Polypeptides, deoxyribonucleic acid (DNA) in helical state, and liquid crystalline polymer (LCP) are well known examples of semiflexible chain. These semiflexible chains also have potential use in controlling surface or interfacial properties through increased brush height. Studies on the flexible chains are mainly based on the random flight statistics[14-17] but the characteristic of the random flight chain is violated by semiflexibility arising from hindrance to internal rotation and structural constraint. This implies that a large number of real polymer chains do not obey the simple statistics of random flight chain (*i.e.*, flexible chain) and consequently other appropriate model is needed. Among a number of models presented for the semiflexible chains, the most well-known model is the worm-like chain proposed by Kratky and Porod[18] in which coarse graining is introduced to replace mathematically intractable discrete chains with continuous models. Several models for both flexible and semiflexible chains are shown in Figure 1. On the other hand, Saito, Takahashi, and Yunoki (STY)[13] have employed the Wiener type integral formulation to provide a functional integral representation for the worm-like chain. In present study, the classical limit mean-field equation for semiflexible polymer brushes is presented by employing a model based on the worm-like chain and the physical properties predicted from the equation are discussed.

Theoretical Model for Semiflexible Polymer Brushes

In order to incorporate semiflexibility in polymer chains,

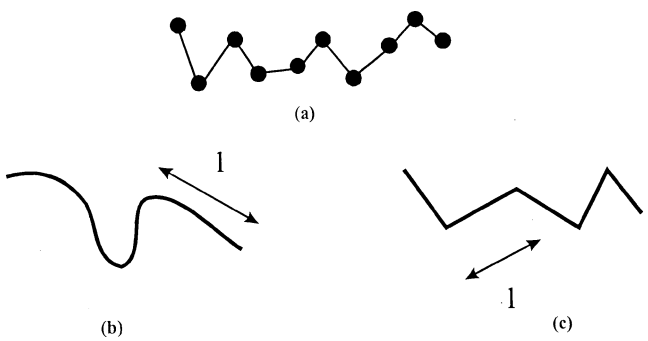

Figure 1. Various models for both flexible and semiflexible polymer chains; (a) Bead-Bond Model, (b) Semiflexible Persistent Chain Model and (c) Semiflexible Freely-Jointed Model.

the Hamiltonian for flexible chains should be modified. In addition to the Wiener form $\beta H = \sum_i \frac{3}{2l^2}\int_0^N d\tau\left(\frac{d\mathbf{r}_i}{d\tau}\right)^2$ accounting for the elastic energy of flexible chains, where $\beta = 1/k_BT$ and $\mathbf{r}_i$ is the position vector of a monomer on ith chain at a contour distance τ along the chain, a curvature (*bending*) energy term which is the second derivative with respect to contour length is introduced to simulate the semiflexibility. This model can be easily extended to more generalized case by incorporating higher derivative terms.[19]

The classical model used to describe the configurational statistics of a semiflexible polymer is the wormlike chain defined by a function given below[13]:

$$Q = \int\prod_i D\mathbf{r}_i\,\tau\exp\left\{-\frac{1}{2l}\beta\varepsilon\sum_i\int_0^N d\tau\left(\frac{d^2\mathbf{r}_i}{d\tau^2}\right)^2\right\} \quad (1)$$

where ε is the bending elastic constant with a dimension of energy per length and the notation $\int D\mathbf{r}_i(\tau)$ denotes the functional integration over all trajectories of the chain, subject to finite chain extensibility constraint $|d\mathbf{r}_i/d\tau|/l = 1$. Unfortunately, for a number of applications the wormlike chain is mathematically cumbersome due to the finite chain extensibility constraint $|d\mathbf{r}_i/d\tau|/l = 1$. As a result, mean-spherical or spherical approximation[20] is introduced to simplify calculations with the model, yet still retaining the essence of semiflexibility of polymer chains. This procedure is, however, analogous to employing the Gaussian model. Consequently, the following mean-spherical Gaussian model is used.

$$Q = \int\prod_i D\mathbf{r}_i(\tau) \quad (2)$$
$$\exp\left\{-\sum_i\frac{3}{2l^2}\int_0^N d\tau\left(\frac{d\mathbf{r}_i}{d\tau}\right)^2 - \frac{1}{2l}\beta\varepsilon\sum_i\int_0^N d\tau\left(\frac{d^2\mathbf{r}_i}{d\tau^2}\right)^2\right\}$$

where the functional integral over $\mathbf{r}_i(\tau)$ is now unconstrained. To model the interactions between polymer brush chains, the osmotic term $\beta H_o = \int d\tau U\left[\mathbf{r}_i(\tau), \frac{d\mathbf{r}_i}{d\tau}\right]$ is introduced, which usually includes anisotropic interactions as well as isotropic interactions between the brush chains.

The self-consistent field equation, which is essentially the Fokker-Planck type equation in the case of a single chain, could be obtained by minimizing the free energy $\beta F = -\ln Q$, which in turn could be solved self-consistently through a propagator G.[19]

$$\left[\frac{\partial}{\partial\tau} - \frac{1}{2\beta\varepsilon l}\nabla_u^2 + l\mathbf{u}\cdot\nabla_r + U\right]G(\mathbf{r},\mathbf{u};\tau) = 0 \quad (3)$$

where $\mathbf{u} = (d\mathbf{r}/d\tau)/l$, U is the dimensionless interaction potential between chain segments, and $\beta\varepsilon l$ represents the chain stiffness which is inversely proportional to the flexibility parameter (α) defined as $\alpha \sim L/\lambda^{-1}$ with L the contour length and λ^{-1} the persistence length.

Most Probable Configuration and Physical Properties of Semiflexible Polymer Brushes

When we deal with long and stretched chains, the distribution of chain configuration is sharply peaked around the most probable configuration (MPC), that is, one which minimizes the exponent of the partition function. In this work, we use the classical limit mean-field approach wherein fluctuations around the most probable path are neglected as polymer chains extend above their Gaussian random coil size. The semiflexible chains generally adopt more stretched configuration due to chain stiffness arising from molecular structures such as mesogenic groups along the liquid crystalline polymer backbone and electronic delocalization of conjugated polymer chains[21] as well as isotropic interaction resulting from the repulsion between segments analogous to flexible polymer brushes. In the case of semiflexible polymer brushes, there also exist anisotropic interactions which are responsible for isotropic-nematic phase transition. However, when we confine semiflexible brushes to a system with only marginal semiflexibility and in a moderately stretched regime, we can simply assume isotropic interactions, meaning that in the regime considered the order parameter, which is defined as $S = 1/2\langle 3\cos^2\vartheta - 1\rangle$ representing the degree of anisotropic interactions arising from chain stiffness and becoming zero for flexible brushes, is almost constant and not of significance in the marginally semiflexible regime considered. By applying the finite chain extensibility through the spherical approximation and employing the Euler-Lagrange equation up to the second order, the most probable configuration for the semiflexible chains was obtained:

$$\frac{3k_BT}{l}\frac{d^2\mathbf{r}}{d\tau^2} - \varepsilon\left(\frac{d^4\mathbf{r}}{d\tau^4}\right) = k_BT\nabla U \quad (4)$$

Without the interaction term ($k_BT\nabla U$), the equation is a fourth-order differential equation describing the bending of a homogeneous rigid rod.[22,23] When we assume that each brush chain is end-tethered normal to the grafting surface, the facts that all the chains are grafted at the same surface and have the same polymerization index N simplify the problem. This means that we use the conventional equal time condition $z = 0$, $(dz/d\tau)/l = -1$ at the grafted end ($\tau = N$) and $z = h$, $d^3z/d\tau^3 = 0$ for the free end ($\tau = 0$). Retaining only dominant terms, the trajectory becomes

$$z = \left(-\frac{1}{\lambda_{++}} + \frac{h|\lambda_{-+}|}{\lambda_{++}}\right)\exp(\lambda_{++}(\tau - N)) - \frac{1}{\lambda_{+-}}\exp(\lambda_{+-}\tau) + \left(\frac{1}{\lambda_{++}} - \frac{h|\lambda_{-+}|}{\lambda_{++}}\right)\sin|\lambda_{-+}|\tau \quad (5)$$
$$+ \left(h + \frac{1}{\lambda_{+-}} + \left(\frac{1}{\lambda_{++}} - \frac{h|\lambda_{-+}|}{\lambda_{++}}\right)\exp(-\lambda_{++}N)\right)\cos|\lambda_{-+}|\tau$$

where $\lambda_{++} = -\lambda_{+-} = ((1/\beta\varepsilon l + ((1/\beta\varepsilon l)^2+8B/\beta\varepsilon l)^{1/2})/2)^{1/2}$, $\lambda_{-+} = i((-1/\beta\varepsilon l + ((1/\beta\varepsilon l)^2+8B/\beta\varepsilon l)^{1/2})/2)^{1/2}$ with $B = \pi^2/8N^2$, and h is the brush height. In the flexible brush limit where $\beta\varepsilon l$ approaches zero, z becomes $h\cos(\tau N/2\pi)$ which is the classi-

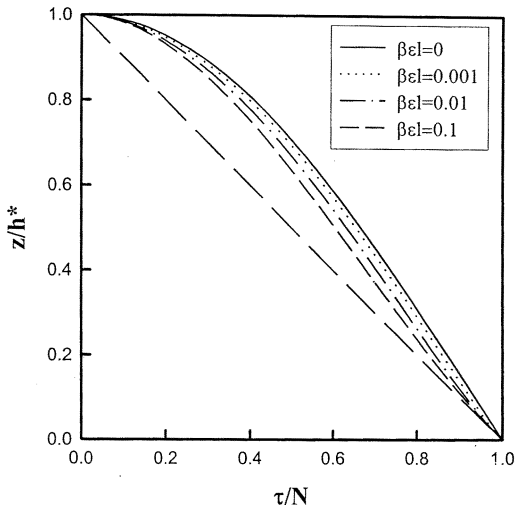

Figure 2. Trajectories of a brush chain normal to a grafting surface with different degrees of chain rigidity ($\beta\varepsilon l$). The solid line indicates the classical limit solution of completely flexible polymer brushes.

cal limit mean-field solution of flexible brushes as shown as a solid curve in Figure 2.[24] For flexible polymer brushes ($\beta\varepsilon l = 0$), the trajectory results in the parabolic density profile of Milner *et al.*[24] while as chain stiffness is increased, the trajectory begins to deviate from the solid curve and asymptotically approaches the diagonal line indicated by the long dashed line in Figure 2 corresponding to a chain trajectory of completely stretched chains. This behavior implies that as chain stiffness is increased, the conformation of brushes gradually changes from a parabolic density profile of completely flexible brushes to a step function density profile for completely stretched brushes, which is in good agreement with a previous study of Wijmans *et al.*[25] in which the self-consistent field (SCF) lattice model was employed. The free energy per chain is obtained from the partition function $\beta F = -\ln Q$ in general. In the classical limit, however, the free energy can be directly derived from the general free energy expression $F \sim \sum_i \frac{3}{2l^2}\int_0^N d\tau\left(\frac{d\mathbf{r}_i}{d\tau}\right)^2 + \frac{1}{2l}\beta\varepsilon\sum_i\int_0^N d\tau\left(\frac{d^2\mathbf{r}_i}{d\tau^2}\right)^2$ by substituting the classical trajectory Eq. (5) into this expression. We also employed the equal time potential of the form $U(z) = A - Bz^2$ with $A(h) = N\sigma\omega/h + Bh^2/3$ and $B = \pi^2/8N^2$ which is obtained from the equal time constraint meaning that all the chains are end grafted at the same surface and have the same polymerization index N[24]. The dominant contribution from the stiffness of chains, after dropping unimportant numerical coefficients, becomes $(\beta\varepsilon l)^{1/2}h/Nl + O(\beta\varepsilon l)$, thus the total free energy obtained can be written as follows:

$$F \sim k_B T\left[\frac{h^2}{Nl^2} - (\beta\varepsilon l)^{1/2}\frac{h}{Nl} + \omega\left(\frac{N^2\sigma}{h}\right)\right] \qquad (6)$$

In the flexible brush limit ($\beta\varepsilon l = 0$), the equilibrium brush height is obtained from minimization of the free energy with respect to brush height resulting in the relation $h^* \sim N(\omega\sigma l^2)^{1/3}$, which is the typical scaling relationship of flexible polymer brushes. When the semiflexibility of a brush chain is considered ($\beta\varepsilon l > 0$), the equilibrium brush height is also obtained from minimization of the free energy with respect to brush height leading to the relation $h^*/l = S + T$, where S and T are

$$S = \left(\frac{\omega\sigma N^3}{4l} + (\beta\varepsilon l)^{3/2}/216 + \left((\omega\sigma N^3)^2/16l^2 + \omega\sigma N^3(\beta\varepsilon l)^{3/2}/432l\right)^{1/2}\right)^{1/3} \qquad (7)$$

$$T = \left(\frac{\omega\sigma N^3}{4l} + (\beta\varepsilon l)^{3/2}/216 - \left((\omega\sigma N^3)^2/16l^2 + \omega\sigma N^3(\beta\varepsilon l)^{3/2}/432l\right)^{1/2}\right)^{1/3} \qquad (8)$$

Because we focus on the scaling relationships the numerical coefficients are not important and could be eliminated from the relations. In the regime where the excluded volume effect is more important than the semiflexibility of brush chains, the equilibrium brush height could be obtained in a simpler form by perturbatively expanding the equilibrium brush height neglecting the higher order terms than $(\beta\varepsilon l)^{1/2}$:

$$h^*/l \sim (\omega\sigma/l)^{1/3}N + (\beta\varepsilon l)^{1/2} \qquad (9)$$

This means that the semiflexibility of a brush chain still contributes to the equilibrium brush height as schematically shown in Figure 3. In the figure, the numerical coefficient is fixed to unity for convenience.

Recently, there have been several studies on the characterization of polymer brushes grafted at solid-liquid interface.[26,27] Klein *et al.*[26] investigated the reduction of frictional force between two solid surfaces bearing polymer brushes using a surface force apparatus. In their experiment, PS chains were end-grafted on mica surfaces in toluene which is a good solvent to PS. The persistent length of the worm-like chain

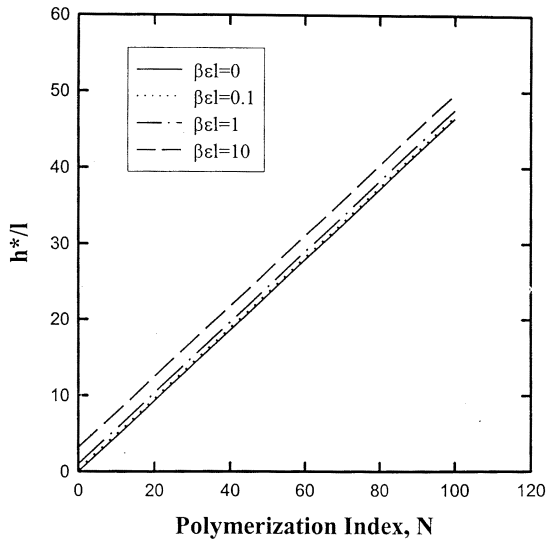

Figure 3. Equilibrium brush height as a function of polymerization index N for different degrees of chain rigidity with $\omega\sigma/l = 0.1$. The brush height should go through the origin regardless of the semiflexibility of a chain in a region close to zero polymerization index. However, each line with a different chain rigidity is drawn in a straight line to show the extrapolated intercept value.

model $(2\lambda)^{-1}$, which is directly proportional to the chain stiffness, is 10.4 for PDMS chain at 25 °C ,while the $(2\lambda)^{-1}$ for PS ranges from 13.2 to 18.8 at 27 °C depending on tacticity,[28] meaning that PS chain is stiffer than PDMS.

Figure 4 illustrates the brush height of end-tethered PS in toluene plotted against PS molecular weight. The linear relationship between brush height and molecular weight is evident and from the best fit, the brush height intercept was estimated to be 21, which is the evidence of semiflexibility contribution to the equilibrium brush height of the PS brushes in the limit of zero molecular weight.

When two particles are brought into a close distance, a strong repulsive force occurs due to the interaction between end-anchored brushes. In steric stabilization of colloidal particles, the interaction between end-tethered brushes plays a crucial role in preventing flocculation in suspension. Using the total free energy

$$F_{com}/k_BT \sim \left[\frac{1}{Nl^2}\left(\frac{h}{h^*}\right)^2 (h^*)^2 - (\beta\varepsilon l)^{1/2}\frac{1}{Nl}\left(\frac{h}{h^*}\right)h^* + \omega N^2\sigma\left(\frac{h^*}{h}\right)\frac{1}{h^*}\right]$$

and the equilibrium brus height $h^*/l \sim (\omega\sigma/l)^{1/3}N + (\beta\varepsilon l)^{1/2}$ the compressional free energy for semiflexible chains is given below, where we neglected the higher order terms than $(\beta\varepsilon l)^{1/2}$:

$$F_{com}/k_BT \sim c_1\left[N\left(\frac{\omega\sigma}{l}\right)^{2/3} + c_2(\beta\varepsilon l)^{1/2}\left(\frac{\omega\sigma}{l}\right)^{1/3}\right]u^2 - c_3 (\beta\varepsilon l)^{1/2}\left(\frac{\omega\sigma}{l}\right)^{1/3}u + N\left(\frac{\omega\sigma}{l}\right)^{2/3}\frac{1}{u} \quad (10)$$

where $u = h/h^*$, h is the compressed brush height, h^* is the equilibrium brush height and c_1, c_2, c_3 are positive numerical constants.

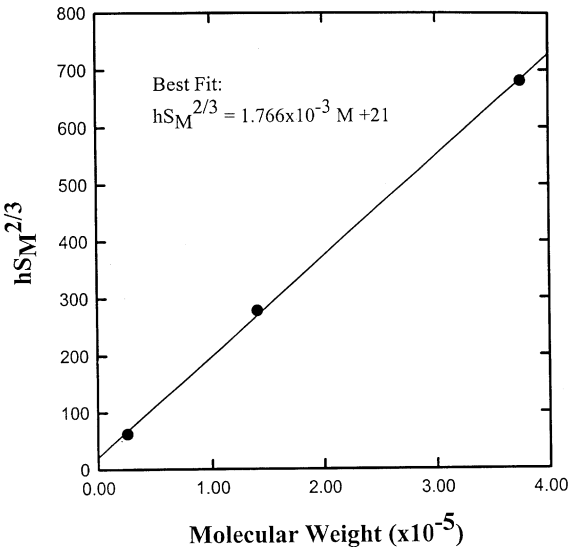

Figure 4. Brush height as a function of PS molecular weight. Data was taken from ref.[25] The brush height scales as $h \sim N\sigma^{1/3}$ in good solvent and the grafting density σ is given by $1/S_M^2$ where N is the chain length, and S_M is the mean inter-anchor spacing. The brush height, rescaled by $S_M^{2/3}$ to remove the grafting density effect, is needed in the ordinate.

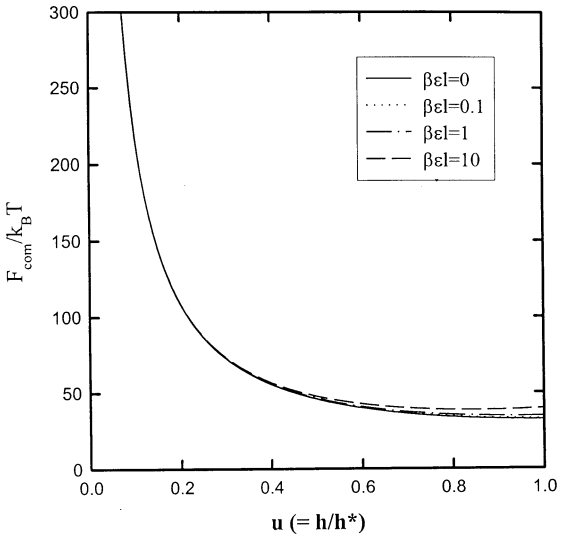

Figure 5. Compressional free energy as a function of u (= h/h^*) for different degrees of chain rigidity with $\omega\sigma/l = 0.1$ and N=100 where h is the compressed brush height and h^* is the equilibrium brush height. The coefficients used in Eq. (10) are $c_1 = 0.5$, $c_2 = 1$, and $c_3 = 0$.

Eq. (10) also shows the effect of chain rigidity on compressional free energy. The first and last terms on the right hand side of Eq. (10) represent contributions to compressional free energy resulting from conformational entropy of the chain and osmotic interactions, respectively, which is the well known form in the case of completely flexible brushes. The second and third terms containing $\beta\varepsilon l$ are the contributions due to chain rigidity. While the second term causes the increase of free energy due to the bending energy of semiflexible chains, the third term decreases the free energy by reducing osmotic interactions since the chain rigidity decreases the conformational entropy of the semiflexible

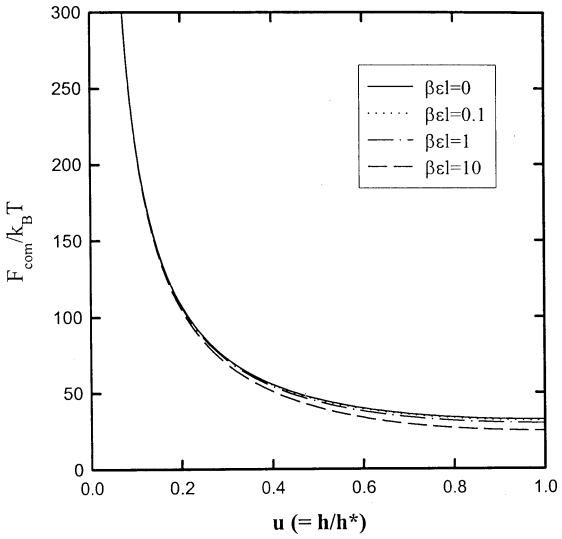

Figure 6. Compressional free energy as a function of u (= h/h^*) for different degrees of chain rigidity with $\omega\sigma/l = 0.1$ and N=100. The coefficients used in Eq. (10) are $c_1 = 0.5$, $c_2 = 10$, and $c_3 = 10$.

chains. Consequently, the actual feature of the resulting compressional free energy depends on relative magnitude of the two rigidity terms with opposite signs. If the decrease of conformatonal entropy due to semiflexibility of chains is negligible, the free energy will exhibit an increased value with increasing chain rigidity. When the third term becomes comparable with the second term in Eq. (10), the compressional free energy decreases with increasing chain rigidity due to the fact that reduced osmotic interactions between semiflexible chains are dominant. The two different cases for the relative magnitude of second and third terms in Eq. (10) are shown in Figures 5 and 6. In Figures 5 and 6, one can notice the abrupt increase of compressional free energy as the compression ratio u becomes smaller. This is due to the term $1/u$ originating from the excluded volume interaction between brush chains,[24] where the compressed brush height h is one half of the separation distance (d) between grafting surfaces, $h \sim d/2$. This excluded volume interaction term yields the typical distance behavior of the free energy of compressed brush layers in the limit of strong compression as shown in Figures 5 and 6.

Summary

The equilibrium properties of *semiflexible* polymer brushes were presented using the classical limit of a mean-field theory for polymer chains with marginal stiffness. The continuous model based on worm-like chain was employed and the most probable path for semiflexible chains was analytically obtained, from which equilibrium brush height as well as interaction between semiflexible brushes was estimated.

References

1. Halperin, A.; Tirrel, M.; Lodge, T. P. *Adv. polym. Sci*. **1991**, *100*, 31.
2. Milner, S. T. *Science* **1991**, *251*, 905.
3. Dolan, A. K.; Edwards, S. F. *Proc. R. Soc. Lond, A*. **1975**, *343*, 427.
4. Donlan, A. K.; Edwards, S. F. *Proc. R. Soc. Lond, A*. **1974**, *337*, 509.
5. Muthukumar, M.; Ho, J. *Macromolecules* **1989**, *22*, 965.
6. Alexander, S. *J. Phys. (Paris)* **1977**, *38*, 977.
7. de Gennes, P.-G. *J. Phys. (Les Ulis, Fr.)* **1976**, *37*, 1443.
8. Lai, P.-Y.; Binder, K. *J. Chem. Phys.* **1991**, *95*, 9288.
9. Lai, P.-Y.; Binder, K. *J. Chem. Phys.* **1992**, *97*, 586.
10. Murat, M.; Grest, G. S. *Macromolecules* **1989**, *22*, 4054.
11. Freed, K. F. *J. Chem. Phys*. **1971**, *54*, 1453.
12. Bawendi, M. G.; Freed, K. F. *J. Chem. Phys*. **1985**, *83*, 2419.
13. Saito, N.; Takahashi, K.; Yunoki, Y. *J. Phys. Soc. Jpn*. **1967**, *22*, 219.
14. Edwards, S. F. *Proc. Phys. Soc*. **1965**, *85*, 613.
15. Helfand, E. *J. Chem. Phys*. **1975**, *62*, 999.
16. Hong, K. M.; Noolandi, J. *Macromolecules* **1981**, *14*, 727.
17. Shull, K. R.; Kramer E. J. *Macromolecules* **1990**, *23*,4769.
18. Kratky, O.; Porod, G. *Rec. Trav. Chim*. **1949**, *68*, 1106.
19. Freed, K. F. *Adv. Chem. Phys*. **1972**, *22*, 1.
20. Ronca, G.; Yoon, D. Y. *J. Chem. Phys*. **1982**, *76*, 3295.
21. Morse, D. C.; Fredrickson, G. H. *Phys. Rev. Lett*. **1994**, *73*, 3235.
22. Courant, R.; Hilbert, D. *Methods of Mathematical Physics*; Interscience Publishers: New York, U. S. A., 1953.
23. Landau, L. D.; Lifshitz, E. M. *Theory of Elasticity*; Pergamon Press: London, U. K., 1959.
24. Milner, S. T.; Witten, T. A.; Cates, M. E. *Macromolecules* **1988**, *21*, 2610.
25. Wijmans, C. M.; Leermakers, F. A. M.; Fleer, G. J. *J. Chem. Phys* **1994**, *101*, 8214.
26. Klein, J.; Kumacheva, E.; Mahalu, D.; Perahia, D.; Fetters, L. J. *Nature* **1994**, *370*, 634.
27. Auroy, P.; Auvray, L.; Leger, L. *Phys. Rev. Lett*. **1991**, *66*, 719.
28. Yamakawa, H. *Ann. Rev. Phys. Chem*. **1984**, *35*, 23.